ISSN: 1692-7257 - Volume 1 – Issue 47 - 2026

ORIGINAL

RCTA
Revista Colombiana de Tecnologías de Avanzada
UNIPAMPLONA

Comparison of color normalization techniques for reduction of tissue heterogeneity in breast cancer histopathological images

Evaluación de técnicas de normalización de color para reducción de heterogeneidad de tejidos en imágenes histopatológicas de cáncer de mama

Diego Andrés Castellano Carvajal[1]
Sergio Alexander Castro Casadiego[2]
Carlos Vicente Niño Rondón[2]
Byron Medina Delgado[2]

[1] **Pontificia Universidad Javeriana, Facultad de Ingeniería y Ciencias, Cali, Valle del Cauca, Colombia.**
[2] **Universidad Francisco de Paula Santander, Departamento de Electricidad y Electrónica, Cúcuta, Norte de Santander, Colombia.**

Received: 01 July 2025. Revised: 01 September 2025. Accepted: 20 December 2025. Published: 01 January 2026.
Corresponding Author: Diego Andrés Castellano Carvajal

How to cite: D. A. Castellano Carvajal, S. A. Castro Casadiego, C. V. Niño Rondón, and B. Medina Delgado, "Evaluación de técnicas de normalización de color para reducción de heterogeneidad de tejidos en imágenes histopatológicas de cáncer de mama", *Revista Colombiana de Tecnologías de Avanzada (RCTA)*, vol. 1, no. 47, ene. 2026, art. no. 4283, doi: 10.24054/rcta.v1i47.4283

This work is licensed under a Creative Commons Attribution-NonCommercial 4.0 International License.

Abstract:

Color normalization in histopathological images is considered an initial step aimed at contributing to consistency in the computational analysis of hematoxylin and eosin (H&E)-stained tissues. In this work, three color normalization methods are evaluated in histopathological images of breast cancer (Macenko, Reinhard, and Vahadane) using quantitative metrics ORB, SSIM, and histogram correlation. In terms of ORB and SSIM, Vahadane stood out for better preserving morphological structures with consistently high values, which is crucial for computational analysis. Nevertheless, Vahadane presented variability in histogram correlation, in contrast to Macenko and Reinhard, who achieved higher and consistent correlations across all samples with average values of 0.9628 and 0.9385. This highlights that the choice of method depends on the balance between structural fidelity and chromatic distribution depending on the case.

Keywords: color normalization, histopathologic imaging, breast cancer.

Resumen:

La normalización del color en imágenes histopatológicas se considera una etapa inicial orientada para contribuir con la coherencia en el análisis computacional de tejidos teñidos con hematoxilina y eosina (H&E). En este trabajo, se evalúan tres métodos de normalización de color en imágenes histopatológicas de cáncer de mama (Macenko, Reinhard y Vahadane) utilizando métricas cuantitativas ORB, SSIM y correlación de histogramas. En términos de ORB y SSIM, Vahadane destacó por preservar mejor las estructuras morfológicas con valores consistentemente altos, lo que es crucial para análisis computacional. No obstante, Vahadane presentó variabilidad en la correlación de histogramas, en contraste con Macenko y Reinhard, quienes lograron correlaciones más altas y consistentes en todas las muestras con valores promedio de 0.9628 y 0.9385. Esto resalta que la elección del método depende del balance entre fidelidad estructural y distribución cromática según el caso.

Palabras clave: normalización de color, imágenes histopatológicas, cáncer de mama.

INTRODUCTION

In recent years, breast cancer has become one of the leading causes of mortality among women worldwide[1]. A significant increase in the incidence of new cases has been observed, even surpassing lung cancer as the most common type of cancer worldwide. In this context, the sentinel lymph node plays a crucial role, as it represents the first metastasis point in the lymph nodes associated with breast cancer. This lymph node receives the primary tumor line, which facilitates the spread of cancer cells[2].

Histopathological images stained with hematoxylin and eosin (H&E) are an important tool in breast cancer diagnosis. However, these images show variability in staining due to differences in reagents and imaging acquisition conditions, which can generate heterogeneity in tissues and affect computational analysis processes and interpretation by pathologists[3].

Various color normalization techniques have been developed to standardize the chromatic appearance of images and facilitate comparison, thereby improving the performance of segmentation models [4] and automated sorting [5]. Among the most commonly used techniques are the methods of Macenko, Reinhard, and Vahadane, which apply different mathematical approaches to adjust the color distribution in images [6].

de Haan et al.[7]they present an innovative deep learning-based framework to transform images of H&E-stained tissues into special stains, such as Masson trichromatic, SBP, and Jones silver staining. This method uses spatially recorded data to train supervised deep neural networks, eliminating dependence on unpaired data. Generating special stains (PAS, Masson-Jones trichrome) from H&E images improved the diagnosis of several non-neoplastic kidney diseases by 22.4%.

Runz et al.[8]investigate the use of CycleGAN (cyclic adversarial generative network) for color normalization in histological images stained with hematoxylin-eosin (H&E) with the aim of reducing variations caused by differences in image acquisition, tissue processing, and staining. Structural similarity index (SSIM) scores indicated high similarity between real images and their reconstructions, with scores above 0.9 for both imaging domains.

Zhao et al.[9]They present RestainNet, a self-directed learning model designed to digitally normalize color spots in pathological images. This innovative model uses a digital grayscale image recoloring process, applying digital hematoxylin (H) and eosin (E) dyes extracted using Beer-Lambert's law. Additionally, a new stain loss function is introduced to ensure dye intensity correction during the retention process. Quantitative comparisons with other methods showed that RestainNet outperforms existing approaches in several parameters. RestainNet scored 0.917 ± 0.019 on the FSIM (Feature Similarity Index), which is higher than other methods. Additionally, in the PSNR (maximum signal-to-noise ratio), RestainNet reached 21,550 ± 3,665, which represents a significant improvement.

Franchet et al.[10]presentan dos nuevas técnicas, AugmentHE y HEnorm, que buscan mitigar el sesgo en la clasificación de imágenes histológicas. Estas técnicas mejoran la precisión y la generalización de los modelos de aprendizaje automático utilizados en patología digital, específicamente en la clasificación histológica del cáncer de mama. Al combinar los conjuntos de datos PACS05 y PACS08, la combinación de HEnorm y augHE mostró un AUC de 0,85 ± 0,02, en comparación con 0,82 ± 0,02 en PACS05 y 0,73 ± 0,07 en PACS08 por separado.

The method proposed by Tosta et al.[11], called SCN-RDL, it focuses on estimating color appearance matrices and spot density maps. Approaches are introduced for pixel selection and weight definition, which improves color estimation. The proposed normalization was evaluated using the DCIS-UDH and UCSB databases. The results showed that the SCN-RDL color normalization method is effective in improving the quality and consistency of hematoxylin and eosin (H&E) stained images, achieving an FSIM (Feature Similarity Index) of 0.9866.

Jeong et al.[12]they develop a scoring-based diffusion model for spot normalization. To avoid confusion in color transfer, they propose a spot separation method that uses scattered non-negative matrix factorization (SNMF) and overlapping moving windows to avoid grid artifacts. The proposed method outperformed conventional methods and those based on generative adversarial networks in several quantitative aspects, showing robustness in unseen data.

Tabatabaei et al.[13]propose a histopathological content-based image retrieval framework (CBHIR) that uses color normalization to improve cancer diagnostic accuracy. The Macenko, Vahadane, and BKSVD techniques were evaluated in the CAMELYON17 dataset, highlighting BKSVD as the most effective, as it achieved a 97% improvement in image retrieval accuracy. The work demonstrates that effective color normalization reduces variability, improves critical image characteristics, and optimizes the performance of computer-aided tools.

This article presents the evaluation and comparison of these three color normalization techniques in histopathological images of lymph nodes with breast cancer. The evaluation uses criteria that measure the preservation of structural and textural features, as well as histogram classification, which allows the chromatic similarity between normalized images to be analyzed.

METHODOLOGY

A three-stage methodology is proposed. In the first stage, the nature of the CAMELYON dataset is analyzed. In the second stage, color normalization methods are applied to the histopathological images. Finally, in the third stage, the effectiveness of the color normalization methods on the histopathological images is compared.

Nature of the CAMELYON dataset

CAMELYON refers to the dataset focused on detecting breast cancer metastases in lymph nodes that contains complete preparation images (WSI) of hematoxylin and eosin stained tissues (H&E) obtained from patient lymph node samples. The images are digitized using high-resolution slide scanners to perform deep cellular-level analysis. For this work, version CAMELYON16 was used, which contains 400 WSI images. They use color depth with red, green, and blue channels, and are stored in TIFF (Tagged Image File Format)[14].

The dataset highlights the variation in image staining caused by differences in H&E staining processes, reagent quality, and digitization parameters, which poses a challenge in automated analysis affecting the performance of segmentation models[15]. Therefore, the CAMELYON dataset is suitable for comparing and evaluating color normalization techniques in terms of standardizing image appearance and reducing the influence of variations. Table 1 presents a summary of the dataset, including technical and descriptive aspects of histopathological images.

Table 1. Technical summary of the CAMELYON16 dataset.

Aspect	Detail
Data type	Digitized histopathological images
Source	Lymph nodes from patients with breast cancer
Resolution	40x (high resolution)
Image format	.tiff (lossless format)
Image size	Approximately 100 000 x 100 000 pixels
Color depth	24 bits (RGB)
Number of slides	400
Staining technique	Hematoxilina y eosina (H&E)

Source: Own elaboration

Techniques for color normalization

For the analysis and comparison of the color normalization methods, a preprocessing step was applied to extract patches, in which each WSI was divided into 1024 x 1024-pixel patches, focusing on regions with relevant tissue and variations in H&E staining.

Macenko

This method proposed by Macenko[16]it is based on separating H&E stains using an optical model and normalizing color intensities. Images are converted from the RGB color space to the optical color space using the Beer-Lambert model to separate stain components, as shown in equation (1), where I is the normalized RGB vector.

$$OD = -\log_{10}(I) \qquad (1)$$

Singular value decomposition is applied to the color intensity matrix to estimate the stain vectors representing the predominant color directions in the image, as presented in equation (2), where OD is the observed optical density value and V and S are the matrices of the stain vectors and the saturations of each of the stains, respectively.

$$S = V^{-1}OD \qquad (2)$$

The color intensities of the original image are projected onto the staining vectors, and the staining intensities are normalized with a linear transformation fitted with the mean and standard deviation of the staining intensities. Finally, the image is reconstructed in the RGB space using the normalized intensities and the staining vectors.

Reinhard

The Reinhard method was implemented[17]to normalize H&E images, where the color distribution of the target image is transferred to the source image in the CIE Lab color space. Initially, the images are converted from RGB to CIE Lab. Next, the averages and standard deviations of the channels are calculated, and for the images. Subsequently, a linear transformation is applied to the pixels of the source image using the means and standard deviations of the reference image, as shown in the equations $l\alpha\beta$ (3), (4) and(5). Finally, the normalized image is converted to RGB space.

$$l' = \frac{\sigma_{l,source}}{\sigma_{l,target}}\left(l - \langle l\rangle_{target}\right) + \langle l\rangle_{source} \qquad (3)$$

$$\alpha' = \frac{\sigma_{\alpha,source}}{\sigma_{\alpha,target}}\left(\alpha - \langle\alpha\rangle_{target}\right) + \langle\alpha\rangle_{source} \qquad (4)$$

$$\beta' = \frac{\sigma_{\beta,source}}{\sigma_{\beta,target}}\left(\beta - \langle\beta\rangle_{target}\right) + \langle\beta\rangle_{source} \qquad (5)$$

Vahadane

The method proposed by Vahadane was implemented[18], which is based on the separation of hematoxylin and eosin (H&E) stains using an optical model and the reconstruction of normalized images. Initially, RGB images are converted to the optical density space OD to linearize the relationship between light intensity and stain concentration, allowing more effective spot separation. Next, a non-negative matrix factorization with dispersion restrictions (SNMF) is used to separate stain spots, as shown in equation (6), where V is the optical density matrix, W contains the color vectors of the spots, and H the density maps.

$$V = WH \qquad (6)$$

The staining concentration matrix is estimated by minimizing a cost function to avoid non-negativity and concentration dispersion, as shown in equation (7), subject to $W, H \geq 0$, where λ is the parameter that controls the dispersion of the intensity maps H.

$$\min_{W,H} \frac{1}{2} \| V - WH \|_F^2 + \lambda \sum_{j=1}^{r} \| H(j,:) \|_1 \qquad (7)$$

The stain concentrations of the original image are normalized with a linear transformation in the concentration space so that they match the mean and standard deviation of the stain concentrations of the target image. The normalized image is reconstructed in the RGB space using the normalized concentrations and the stain matrix of the reference image to preserve the tissue structures with a standardized color distribution, as shown in equation (8), where $V_{norm} = W_t H_s^{norm}$, W_t is the color vector matrix of the target image and H_{norm}^S is the normalized density map matrix of the source image.

$$I_{norm} = I_o exp(-V_{norm}) \qquad (8)$$

Evaluation criteria

ORB (Oriented Fast and Rotated Brief) is a detection and descriptor algorithm used to compare features between histopathological images before and after normalization, in order to evaluate the normalized image in terms of preservation of tissue and cellular structures. ORB combines two main components: FAST (Features from Accelerated Segment Test), a point detector for identifying regions of interest in the image based on pixel intensity, and BRIEF (Binary Robust Independent Elementary Features), a descriptor used to represent the detected features.

The structural similarity index (SSIM) is an image similarity metric based on luminance, contrast and structural components, which takes human visual perception into account to evaluate the quality of medical images and quantify the structural similarity between the original and normalized images. Equation (9) describes the metric, where μ_x and μ_y are the means of images x and y, σ_x^2 and σ_y^2 are the variances of images x and y, σ_{xy} is the covariance between x and y, and C_1 and C_2 are the constants that prevent division by zero.

$$SSIM(x,y) = \frac{(2\mu_x\mu_y + C_1)(2\sigma_{xy} + C_2)}{(\mu_x^2 + \mu_y^2 + C_1)(\sigma_x^2 + \sigma_y^2 + C_2)} \qquad (9)$$

The statistical correlation method was also used to analyze the distribution histograms generated by each grayscale image. In this case, H1, H2, H3 and H4 represent the histograms corresponding to the original image, the image normalized by the Macenko method, the image resulting from the Reinhard method and the image obtained with the Vahadane method, respectively. These histograms were normalized in the same scale space to facilitate the comparison of similarity between the images.

Correlation with descriptive statistics (mean, standard deviation, minimum and maximum) was applied to determine the relationship between the histograms, obtaining values in the range of -1 to 1. A value close to 1 indicates a perfect direct correlation, whereas a value close to -1 suggests a perfect inverse correlation. A value close to 0, in turn, implies that there is no correlation between the variables. Equation (10) describes the methodology used to calculate the point-to-point correlation from the values obtained in the histograms.

$$d(H_1, H_{2,3,4}) = \frac{\Sigma_I \left(H_1(I) - \overline{H}_1\right)\left(\overline{H}_{2,3,4}(I) - \overline{H}_{2,3,4}\right)}{\sqrt{\Sigma_I \left(H_1(I) - \overline{H}_1\right)^2 * \Sigma_I \left(H_{2,3,4}(I) - \overline{H}_{2,3,4}\right)^2}} \qquad (9)$$

RESULTS AND DISCUSSION

Based on the proposed methodology, figure 1 presents the preprocessing performed on the images of the CAMELYON16 dataset resized to 1024 x 1024 pixels, where section A shows the images in RGB representation, section B shows the target image that is representative of the dataset and captures the typical features of the staining (hematoxylin and eosin intensity). Section C shows the Macenko normalization, in D the

Reinhard normalization and in E the Vahadane normalization.

Similarly, figure 2 shows the histograms obtained in each of the five test images for the validation of the color normalization methods for H&E images, where the redistribution of the color channels and the variations between the histograms that represent

the adjustments suggested by each model can be observed as a function of the sensitivity to staining or illumination differences. The histograms corresponding to A, B and E showed better consistency in the intensity distribution after normalization. This was reflected in a more uniform distribution of the intensity values, with well-defined peaks and less dispersion in the color channels (hematoxylin and eosin). In contrast, histograms C and D showed greater variability in the intensity distribution. This could be due to differences inherent to the original staining of these images, such as excessive or insufficient staining, or the presence of artifacts that hindered normalization.

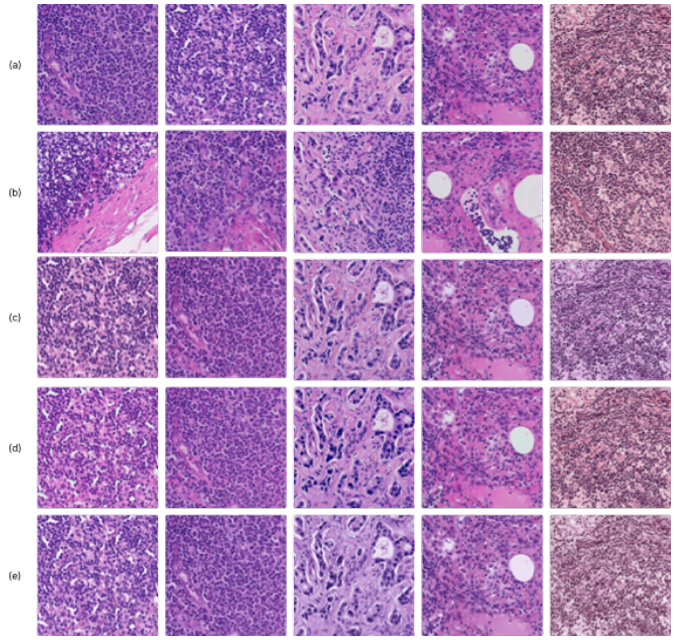


Fig. 1. *Color normalization of the H&E images from CAMELYON16*
Source: Own elaboration

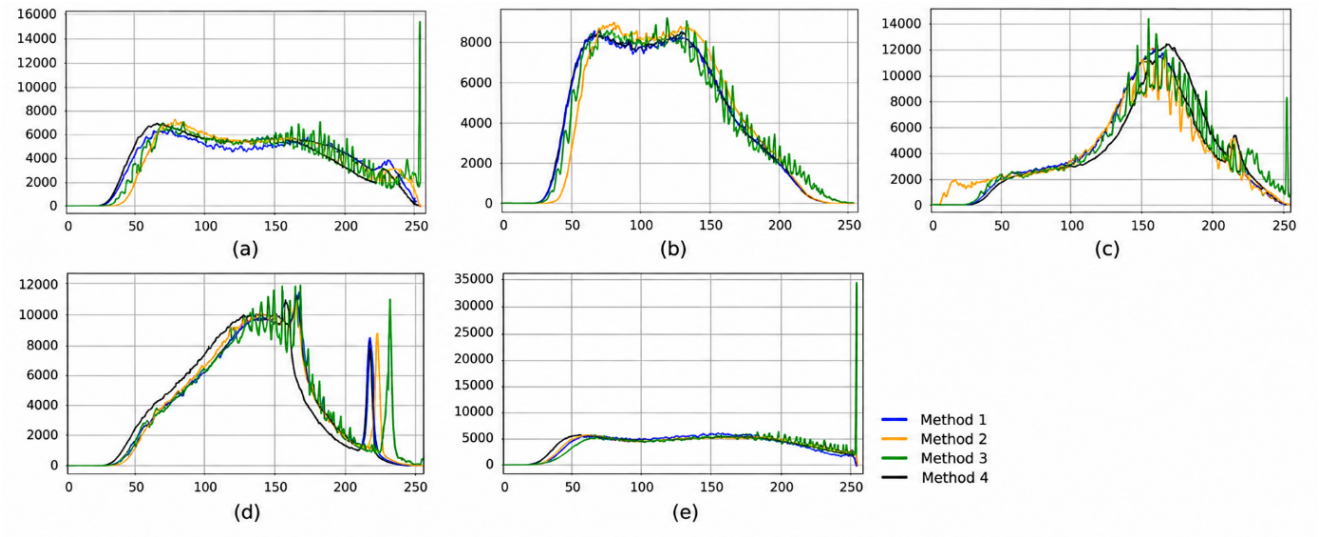


Fig. 2. *Histogram obtained for the sample images*
Source: Own elaboration

Table 2 presents the correlation values and the descriptive statistics among the three normalization methods for histopathological images: Macenko, Reinhard and Vahadane.

Five samples representing histopathological images from different patients or tissues were evaluated. In sample 1, Macenko and Reinhard show a high correlation of 0.9540 and 0.9038, respectively, whereas Vahadane has a lower correlation, with a value of 0.8213. In sample 5, by contrast, Vahadane shows a significantly lower correlation compared with Macenko and Reinhard.

It should be noted that Macenko and Reinhard show consistently high correlation values across all samples, suggesting that

these methods produce similar results in color normalization. Vahadane, although a more advanced method, shows a more variable correlation. In particular, in sample 5, the correlation is significantly lower, which could indicate that this method does not fit certain types of images or fabrics well[19].

The variability in the correlation values suggests that the choice of normalization method may depend on the type of tissue or on the specific features of the image. In terms of descriptive statistics, Macenko has the highest mean, with a value of 0,9628, and the lowest standard deviation, with 0,0189, which indicates that it is the most consistent and reliable method in terms of correlation. Reinhard also shows a high mean (0,9385) and a moderate standard deviation (0,0316), which suggests that it is a robust method[20], although slightly less consistent than Macenko. Vahadane has the lowest mean, with 0,8281, and the highest standard deviation (0,1811), which demonstrates greater variability in its performance. This suggests that, although it may perform very well in some cases (for example, in sample 2), in other cases its performance is significantly lower (for example, in sample 5).

Table 2. Correlation values and descriptive statistics by normalization method

Sample	Macenko	Reinhard	Vahadane	Statistics	Macenko	Reinhard	Vahadane
Sample 1	0.9540	0.9038	0.8213	Mean	0.9628	0.9385	0.8281
Sample 2	0.9994	0.9677	0.9851	Standard deviation	0.0189	0.0316	0.1811
Sample 3	0.9549	0.9223	0.9359	Minimum	0.9508	0.9038	0.5130
Sample 4	0.9508	0.9197	0.8853	Maximum	0.9994	0.9791	0.9851
Sample 5	0.9547	0.9791	0.5130				

Source: Own elaboration

Similarly, figure 3 shows the box plots comparing the distributions of the normalization methods for the ORB and SSIM metrics. For the ORB analysis, the Macenko method produces high values in some areas and tends to generate a less uniform color distribution (high dispersion). Its median is slightly lower than that of the other techniques, and the intensity values are lower, which affects the visual interpretation of the normalized images. In addition, its performance is less stable and consistent. Reinhard shows a median slightly higher than that of Macenko, and its values are more clustered, which indicates greater stability in the results. Vahadane also presents a slightly high median and has less dispersion than Macenko, which shows greater consistency. On the other hand, in the SSIM analysis, Macenko presents a high median, which indicates that, in most cases, the normalized images are similar to the reference image.

In addition, it presents a low dispersion and does not show significant variations between images, which demonstrates greater consistency. Reinhard showed a greater dispersion, and the normalized images vary more widely, due to its sensitivity to differences in the images and its dependence on the statistical color values. The method is not as consistent as Macenko, and its performance may be acceptable for some images, but less effective for others. Overall, the quality of normalization with Reinhard is acceptable and does not surpass that of Macenko. On the other hand, Vahadane has a median close to that of Macenko, and its dispersion is low, which indicates stability among the values.

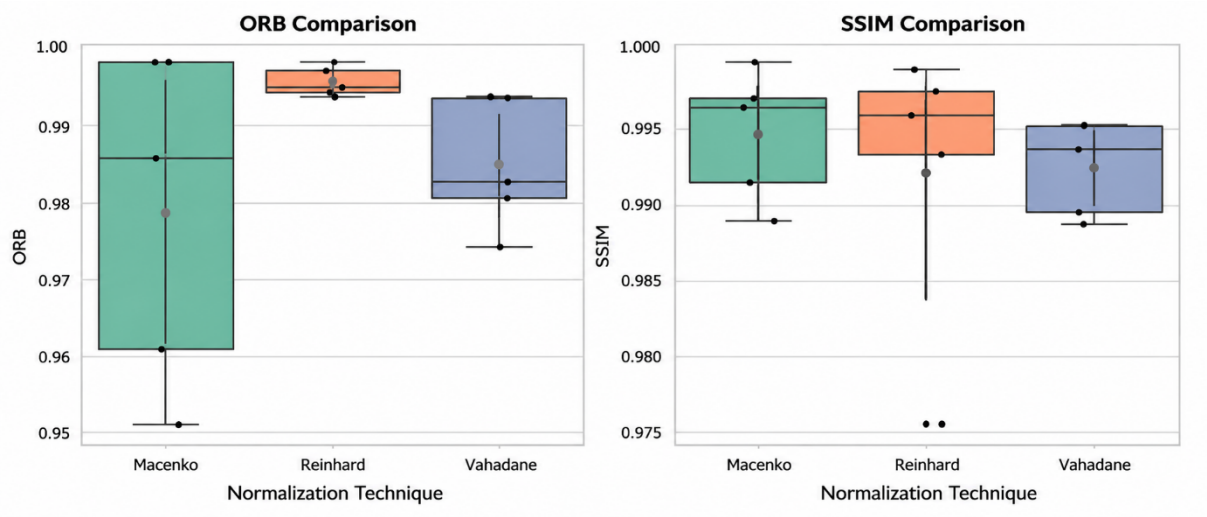


Fig. 3. *Box plot of the ORB and SSIM metrics*
Source: Own elaboration

CONCLUSIONS

Three color normalization techniques, Macenko, Reinhard and Vahadane, were compared on histopathological images stained

with hematoxilina y eosina (H&E) of lymph nodes with breast cancer. For the evaluation, histogram correlation and ORB and SSIM similarity metrics were used, which allow measuring the consistency in color distribution and the structural similarity between the normalized images and their original versions. The results obtained indicate that Vahadane is the technique with the best overall performance, since it presented higher values and lower variability in ORB and SSIM, which suggests greater stability and fidelity in the preservation of the morphological features of the tissues, which is crucial for computational analysis applications, such as automated segmentation and classification, where the preservation of cellular and tissue structures contributes to model accuracy. However, the histogram correlation results showed that Vahadane presents significantly lower values compared with Macenko and Reinhard. Although this technique better preserves the structure and texture patterns of the images, it modifies the hues and color distribution more, generating images with more significant chromatic differences compared with the original. Conversely, Macenko and Reinhard preserve greater similarity in color distribution, but with a slight loss in structure preservation. The comparison provides information to improve standardization in the processing of histopathological images, which can have a positive impact on computer-aided diagnosis and on the development of artificial intelligence models applied to digital pathology.

REFERENCES

[1] C. Kaushal, S. Bhat, D. Koundal, and A. Singla, "Recent Trends in Computer Assisted Diagnosis (CAD) System for Breast Cancer Diagnosis Using Histopathological Images," *IRBM*, vol. 40, no. 4, pp. 211–227, Aug. 2019, doi: 10.1016/j.irbm.2019.06.001.

[2] S. yang Tang, L. Li, Y. lin Li, A. yuan Liu, M. jun Yu, and Y. ping Wan, "Distribution and location of Daxx in cervical epithelial cells with high risk human papillomavirus positive," *Diagn Pathol*, vol. 9, no. 1, Jan. 2014, doi: 10.1186/1746-1596-9-1.

[3] F. Li, J. Ma, T. Wen, Z. Tian, and H. N. Liang, "HI-Net: A novel histopathologic image segmentation model for metastatic breast cancer via lightweight dataset construction," *Heliyon*, vol. 10, no. 19, p. e38410, Oct. 2024, doi: 10.1016/J.HELIYON.2024.E38410.

[4] A. Agrawal and V. Maan, "Enhanced Brain Tumor Segmentation and Size Estimation in MRI Samples using Hybrid Optimization," *Data and Metadata*, vol. 3, pp. 408–408, Jan. 2024, doi: 10.56294/DM2024408.

[5] G. A. Ansari, S. S. Bhat, M. D. Ansari, S. Ahmad, and H. A. M. Abdeljaber, "Prediction and Diagnosis of Breast Cancer using Machine Learning Techniques," *Data and Metadata*, vol. 3, p. .346-.346, Sep. 2024, doi: 10.56294/DM2024.346.

[6] T. A. Azevedo Tosta, P. R. de Faria, L. A. Neves, and M. Z. do Nascimento, "Computational normalization of H&E-stained histological images: Progress, challenges and future potential," *Artif Intell Med*, vol. 95, pp. 118–132, Apr. 2019, doi: 10.1016/J.ARTMED.2018.10.004.

[7] K. de Haan et al., "Deep learning-based transformation of H&E stained tissues into special stains," *Nat Commun*, vol. 12, no. 1, Dec. 2021, doi: 10.1038/s41467-021-25221-2.

[8] M. Runz, D. Rusche, S. Schmidt, M. R. Weihrauch, J. Hesser, and C. A. Weis, "Normalization of HE-stained histological images using cycle consistent generative adversarial networks," *Diagn Pathol*, vol. 16, no. 1, Dec. 2021, doi: 10.1186/s13000-021-01126-y.

[9] B. Zhao et al., "RestainNet: A self-supervised digital re-stainer for stain normalization," *Computers and Electrical Engineering*, vol. 103, Oct. 2022, doi: 10.1016/j.compeleceng.2022.108304.

[10] C. Franchet et al., "Bias reduction using combined stain normalization and augmentation for AI-based classification of histological images," *Comput Biol Med*, vol. 171, Mar. 2024, doi: 10.1016/j.compbiomed.2024.108130.

[11] T. A. A. Tosta, A. D. Freitas, P. R. de Faria, L. A. Neves, A. S. Martins, and M. Z. do Nascimento, "A stain color normalization with robust dictionary learning for breast cancer histological images processing," *Biomed Signal Process Control*, vol. 85, Aug. 2023, doi: 10.1016/j.bspc.2023.104978.

[12] J. Jeong, K. D. Kim, Y. Nam, C. E. Cho, H. Go, and N. Kim, "Stain normalization using score-based diffusion model through stain separation and overlapped moving window patch strategies," *Comput Biol Med*, vol. 152, Jan. 2023, doi: 10.1016/j.compbiomed.2022.106335.

[13] Z. Tabatabaei, F. Pérez Bueno, A. Colomer, J. O. Moll, R. Molina, and V. Naranjo, "Advancing Content-Based Histopathological Image Retrieval Pre-Processing: A Comparative Analysis of the Effects of Color Normalization Techniques," *Applied Sciences (Switzerland)*, vol. 14, no. 5, Mar. 2024, doi: 10.3390/app14052063.

[14] E. Bütün, M. Uçan, and M. Kaya, "Automatic detection of cancer metastasis in lymph node using deep learning," *Biomed Signal Process Control*, vol. 82, p. 104564, Apr. 2023, doi: 10.1016/J.BSPC.2022.104564.

[15] M. Veta, P. J. van Diest, R. Kornegoor, A. Huisman, M. A. Viergever, and J. P. W. Pluim, "Automatic Nuclei Segmentation in H&E Stained Breast Cancer Histopathology Images," *PLoS One*, vol. 8, no. 7, p. e70221, Jul. 2013, doi: 10.1371/JOURNAL.PONE.0070221.

[16] M. Macenko et al., "A method for normalizing histology slides for quantitative analysis," Proceedings - 2009 IEEE International Symposium on Biomedical Imaging: From Nano to Macro, ISBI 2009, pp. 1107–1110, 2009, doi: 10.1109/ISBI.2009.5193250.

[17] E. Reinhard, M. Ashikhmin, B. Gooch, and P. Shirley, "Color transfer between images," *IEEE Comput Graph Appl*, vol. 21, no. 5, pp. 34–41, Sep. 2001, doi: 10.1109/38.946629.

[18] A. Vahadane et al., "Structure-Preserving Color Normalization and Sparse Stain Separation for Histological Images," *IEEE Trans Med Imaging*, vol. 35, no. 8, pp. 1962–1971, Aug. 2016, doi: 10.1109/TMI.2016.2529665.

[19] A. Sethi et al., "Empirical comparison of color normalization methods for epithelial-stromal classification in H and E images," *J Pathol Inform*, vol. 7, no. 1, p. 17, Jan. 2016, doi: 10.4103/2153-3539.179984.

[20] S. Roy, S. Panda, and M. Jangid, “Modified Reinhard Algorithm for Color Normalization of Colorectal Cancer Histopathology Images,” 2021 29th European Signal Processing Conference (EUSIPCO), pp. 1231–1235, Aug. 2021, doi: 10.23919/EUSIPCO54536.2021.9616117.

FUNDING

No financing

CONFLICT OF INTEREST

None

AUTHORSHIP CONTRIBUTIONS

Drafting – original draft: Diego Andrés Castellano Carvajal, Sergio Alexander Castro Casadiego, Carlos Vicente Niño Rondón, Byron Medina Delgado.

Writing–review and editing: Diego Andrés Castellano Carvajal, Sergio Alexander Castro Casadiego, Carlos Vicente Niño Rondón, Byron Medina Delgado.